NPL Report CBTLM4

REPORT

Experimental verification of a swept-frequency laser interferometer for distance measurement

C. S. Edwards, P. Gill and P. Taylor

January 2000

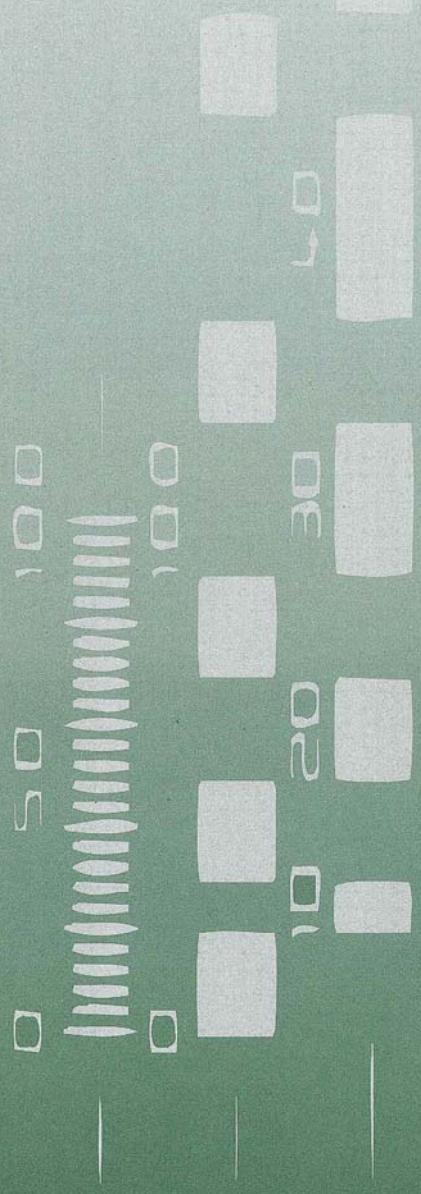

NPL
National Physical Laboratory

National Physical Laboratory is operated on behalf of the DTI by NPL Management Limited, a wholly owned subsidiary of Serco Group plc

NPL Report CBTLM4

January 2000

Experimental verification of a swept-frequency laser interferometer for distance measurement.

C. S. Edwards, P. Gill and P Taylor

Centre for Basic, Thermal and Length Metrology
National Physical Laboratory,
Queens Road, Teddington, Middlesex TW11 0LW, UK

Abstract

A swept-frequency Michelson interferometer system has been developed, based on a tunable visible laser diode with a stable Fabry-Pérot cavity as a frequency sweep reference. Its performance has been verified by direct comparison with a displacement-measuring laser interferometer for path differences in the range 1 m to 20 m. The best fractional uncertainty of 3.2×10^{-6} is achieved at a distance of 8 m. The limitations of the technique are discussed, along with the scope for further improvements.

© Crown Copyright 2000
Reproduced by permission of the Controller of HMSO

ISSN 1469-4921

Extracts from this report may be reproduced provided the source is acknowledged and the extract is not taken out of context

Authorized for publication on behalf of the Managing Director of NPL by Dr David Robinson
(Head of the Centre for Basic, Thermal and Length Metrology)

Contents

1. Introduction

There is considerable current interest in the technique of swept-frequency interferometry for length and distance metrology [1-14]. The advent of single-longitudinal mode diode lasers, with their wide tunability, has opened up new possibilities for this technique, and accuracies of a few parts in 10^{10} have been reported for measurements of a stable Fabry-Pérot structure in a vacuum [14]. This paper describes the development of a swept-frequency Michelson interferometer system for more general distance measurement. The system uses a commercially available visible laser diode system (centre wavelength ~ 636 nm) which is capable of a continuous frequency sweep of approximately 6 THz. The interference fringes of a stable Fabry-Pérot cavity of known free spectral range are used to calibrate the frequency sweep. The use of visible radiation facilitates rapid alignment of the interferometer, and the close proximity to the 633 nm HeNe wavelength permits the use of standard interferometer optics. The swept-frequency interferometer is evaluated by direct comparison against a traceable bi-directional fringe-counting laser interferometer and its statistical and systematic errors are characterized.

2. Principles of the swept-frequency interferometer

In order to discuss swept-frequency interferometry and its application to precision length measurements, it is useful to consider the case of a laser aligned into an interferometer of free spectral range ν_{FSR}. If the output of the laser is swept through a frequency range $\Delta\nu$, N fringes are generated at the output of the interferometer. Provided the frequency scan range is accurately known, the free spectral range and hence the optical path length of the interferometer may be determined by counting the number of fringes. For a Michelson or mode-matched Fabry-Pérot interferometer, the path length L is given by

$$L = \frac{N.c}{2n.\Delta\nu} \tag{1}$$

where c is the speed of light in vacuo and n is the refractive index in the medium of propagation.

In the system described in this paper, the laser output is split into two and these beams are aligned into two separate interferometers. The first of these is a Michelson interferometer, and the path difference between the reference arm and the measuring arm of this system constitutes the "distance" to be measured. The other interferometer is a stable Fabry-Pérot cavity housed in a temperature-controlled vacuum chamber. As the laser frequency is swept, the Michelson interferometer gives a sine wave output, converted by signal processing electronics into a pulse train with two pulses per fringe. At the same time, the Fabry-Pérot also gives an analogue pulse train output, converted to digital pulses by signal-processing electronics. By counting an exact number N_{FP} of Fabry-Pérot pulses and using these to gate the Michelson signal, one obtains a Michelson fringe count N_F, accurate to the nearest half fringe, corresponding to the frequency interval $\Delta\nu = N_{FP} \times \nu_{FSR}$. Thus the equation for the path length becomes:-

$$L = \frac{N_F.c}{2n.N_{FP}.\nu_{FSR}} \tag{2}$$

Thus if ν_{FSR} is known, L can be determined. The limitations on accuracy are set by the count statistics and by the type B uncertainties associated with the assumed value of ν_{FSR} and the sensor-related uncertainty in the derivation of n from Edlén's equations [15, 16]. As L is proportional to the Michelson fringe count N_F, the fractional resolution of the distance measurement is expected to improve with distance i.e. the fractional uncertainty should decrease as the measurement distance increases.

3. Determination of the Fabry-Pérot free spectral range

The extended cavity laser used in this work is a commercially available device (New Focus Model 6305). This uses an anti-reflection coated laser diode in a Littman configuration extended cavity design [17], which gives a large continuous tuning range, in this case from 468.8 THz to 474.7 THz. The output power is a few mW over this range (Fig. 1). The laser can be tuned either by a piezo-electric transducer (PZT) for short range tuning (up to 100 GHz) or by a stepper motor for a longer range scan. In addition to the diode's broad gain curve, some additional amplitude modulation is apparent (Fig. 1). This arises from the residual reflectance of the diode's front facet and has a period of ~ 50 GHz, corresponding to the optical cavity length of the laser diode chip. The short term (≤ 1 s time-scale) spectral linewidth of the laser has been determined to be ~ 1 MHz by beat frequency comparison with a HeNe laser. Assuming this linewidth is Lorentzian in form, this gives an estimated coherence length of ~ 100 m [18].

The Fabry-Pérot reference cavity is a spherical mirror, non-confocal design, with a mirror separation of ≈ 100 mm and a finesse of ~ 1000. The mirrors are optically contacted onto a spacer of ultra-low-expansion material and the cavity is housed in a temperature-controlled vacuum chamber. The pressure in the chamber is ~ 10^{-3} Pa and the temperature variation is less than ±50 mK. This design of cavity has been evaluated over a period of a few years, and typically displays a coefficient of thermal expansion of a few parts in 10^8 per Kelvin, and an isothermal drift of a few parts in 10^{12} per day [19]. Thus its stability is more than adequate to permit 1 part in 10^6 fractional length accuracy.

The experimental set-up used to measure the Fabry-Pérot free spectral range ν_{FSR} is shown in Fig. 2. The diode laser was frequency modulated via its injection current at a frequency of 7.2 kHz to a peak-to-peak modulation depth of 5 MHz. Light from the laser was passed through an optical isolator (30 dB isolation), spatially filtered and then mode-matched into the cavity, and the fringes were detected using a phase-sensitive detector. This provided a locking discriminant to which the laser was frequency stabilized by the integrator feeding back to the PZT. Light from the diode laser was also mixed with the output of a HeNe reference laser (NPL-D) stabilized to a hyperfine component of the 11-5, R(127) transition of iodine at 473.6 THz [20] and the resultant beat was detected with a broad bandwidth (5 GHz) Si PIN photodiode. A double-balanced-mixer was used with a radio frequency synthesizer to down-shift the beat frequency to a more convenient range for filtering and counting.

The measurement procedure was as follows. The diode laser was locked to a fringe of order N_0 a few GHz lower in frequency than the HeNe, and the beat frequency measured for a 20 s averaging time. The measurement was then repeated with the diode laser locked to the fringe of order $(N_0 + 4)$, a few GHz higher in frequency than the HeNe. Summing the absolute values of the two beat frequencies (taking into account the synthesizer mixing frequency) thus yielded a value of $4 \times \nu_{FSR}$. This measurement was repeated 35 times over a period of two days. The overall mean value of ν_{FSR} was found to be 1 488 074.7 kHz, with a standard

uncertainty of 520 Hz. This corresponds to a fractional uncertainty of 3.5×10^{-7}. In order to ensure traceability to national standards, the synthesizer and the counter were both calibrated using an off-air frequency standard capable of an accuracy of 2 parts in 10^9 for a 10 s measurement period.

4. Length measurement and accuracy verification

The experimental set-up used for the distance measurements is shown in Fig. 3. The output from the diode laser passes through a beam expander and approximately 10% is directed into the swept-frequency Michelson interferometer. This interferometer is based on a design described elsewhere [21]. Its beamsplitter assembly consists of a pair of identical wedged glass plates. The first surface of the first plate (P1) has a thin metallic coating which gives a 30/30 splitting ratio (transmitted power/reflected power, by percentage), with a 90° phase shift between the two outputs, with both phase and intensity independent of the incident polarization. P2 is an uncoated compensating plate oriented so as to cancel the angular deviation resulting from the wedge of P1. Retroreflectors R1 and R2 form the two arms of the Michelson interferometer.

For the purposes of direct comparison, a bi-directional fringe-counting displacement interferometer [22] is set up with the same measurement axis. Both interferometers are Abbe compensated about the measurement axis in the same plane. This NPL reference interferometer is capable of displacement measurements up to 50 m with an accuracy of $\pm 1.6 \times 10^{-7}$, with direct traceability to UK national standards. For the purposes of this comparison, R1 and R3 are fixed, while R2 and R4 are mounted together on a moving carriage, capable of traversing distances of up to 50 m. The apparatus is housed in a temperature-controlled laboratory (control temperature 18.0 ± 0.4°C).

A simplified schematic of the swept frequency interferometer electronics is shown in Fig. 4. In essence, during the laser frequency sweep the Fabry-Pérot fringe signal is used to gate the Michelson fringe signal for a period corresponding to a precise and predetermined frequency sweep range. This range can then be used with the observed number of Michelson fringes N_F to determine the length of the measurement arm.

As can be seen from Fig. 1, the output power of the diode laser varies considerably over the frequency scan, giving a Michelson fringe size varying by a factor of 2. The fringe equalization electronics uses a process of analogue division, with the reference photodiode PD2 providing the denominator input, to reduce the fringe intensity variation in both interferometer signals to $\approx$ 10% peak-to-peak.

The Michelson signal is fed into the signal processing electronics, where it is converted from a sine wave to a square wave by comparator 1, and is then fed into monostable multivibrator 1. This is used to "lock out" false count events caused by noise on the Michelson fringe signal, and provides pulses on both the upward and downward going edges of the square wave i.e. two pulses per fringe. The output pulse width is switchable over the range 0.5 μs to 40 μs to enable its use for a variety of distances and scan speeds. The ouput from the signal processing electronics is fed through an AND gate to a counter.

The Fabry-Pérot pulse train is converted from analogue to digital by comparator 2 and a monostable multivibrator, and this pulse train is then fed into the cascaded down counters 1 and 2. These control the AND gate. Counter 1 sets a "pre-count" value of Fabry-Pérot fringes. This acts to "lock out" the Michelson signal during the early stages of the laser scan, when the scan rate is changing rapidly and the laser frequency is at its noisiest, by counting Fabry-Pérot fringes until a programmed number N_{PC} is reached. At this point it opens the AND gate and

the fringe counter starts counting pulses from the Michelson signal processing electronics. This continues until Counter 2 reaches its preset value N_{FP}, at which point the AND gate closes to give N_F. This concludes the measurement cycle.

For the data described in this paper, N_{PC} was chosen to be 700 and N_{FP} was 2000. The count period thus corresponded to a frequency sweep of $2000 \times \nu_{FSR}$, i.e. 2 976 149.4 (1.0) MHz. Calibrated air temperature, pressure and humidity sensors were placed along the measurement path, and Edlén's equations [15, 16] were used to calculate refractive index n. The distance was then calculated from equation (2). Ten measurements were made at each distance and averaged to give a mean value and uncertainty. This uncertainty value was then combined with the type B contributions from ν_{FSR} and n (fractional uncertainties of 3.5×10^{-7} and 0.5×10^{-7} respectively, this latter resulting from air sensor errors) to give an overall estimated uncertainty at each distance. Prior to the measurements, the alignment of both interferometer systems was checked over a distance of 50 m to ensure the cosine error was negligible (estimated < 1 part in 10^9).

5. Results and discussion

The results of the displacement comparison between the two interferometers are shown in Fig. 5. The displacement of "0 m" for the NPL reference interferometer corresponds to a distance of 1.163 931 m for the swept-frequency interferometer. This distance is subtracted from the longer distance values to give displacements. As is clear from Fig. 5, the system performs in line with expectations up to a displacement of ~ 6.5 m, at which point the fractional uncertainty of the distance measurement is 3.2×10^{-6}. For these first few displacement values, the residuals are small and not statistically significant (averaging 0.8 parts in 10^6 with a fractional uncertainty of 4.9 parts in 10^6) and the fractional uncertainty is seen to decrease with distance. The measurement accuracy is limited by the system's resolution (half a Michelson fringe) at these distances and could in principle be improved by further fringe subdivision (in practice the limitations of the laser system, discussed below, prevented this). Beyond this point, the fractional uncertainty increases and the swept-frequency interferometer begins to systematically over-estimate the distance, despite the relatively good statistics. This illustrates the benefit of verifying this system's performance by direct comparison against an independent measurement technique; an accuracy estimation based solely on the estimated uncertainty or by comparing results for some small displacement at a large distance would over-estimate the accuracy by as much as an order of magnitude.

The observed systematic error corresponds to the counting electronics consistently miscounting high. The probable causes of this miscount arise from the limitations of the commercial laser system used in this work. There are two main contributing factors. Firstly, the laser is scanned by a stepper motor and so at low scan speeds the laser frequency is scanned as a series of discrete steps. In order to counter this problem, the laser was scanned comparatively quickly at rates of up to 3 THz/s, and at these high rates the scan becomes continuous and monotonic. Even so, the laser output is frequency-modulated during the scan and the frequency of the sine wave output from the Michelson interferometer varies by a factor of ~ 2. This frequency variation makes it difficult to select an ideal monostable output pulse width. The second contributing factor is the mechanical "jitter" of the laser frequency during the scan, which imposes a second comparatively "fast" frequency modulation on the laser output. At short distances, where the Michelson free spectral range is large compared to the laser frequency excursions, this is not expected to be a problem, as the interferometer will

simply convert laser frequency noise into amplitude noise. However, when the laser jitter of a few MHz peak-to-peak becomes a sizeable fraction of the interferometer's free spectral range, then the deviations from monotonic scanning may well give rise to false count events. This seems the most probable cause of the problem encountered at distances beyond 8 m (i.e. for free spectral ranges ≤ 20 MHz). The amplitude modulation of the laser output (Fig. 1) is largely suppressed by the analogue division electronics and thus is not expected to degrade the measurement accuracy.

If the linearity of the scanning was improved, and the acoustic jitter of the laser reduced, further fringe subdivision could be implemented. The system accuracy would then be limited by problems arising from variation in the optical path length of the interferometer measurement arm during the period of the scan. At longer distances (greater than 10 m), the fringe count can slip by one or two fringes due to a change in this length, predominantly due to variation in the refractive index of the air. Observations of the change in the fringe-count of the NPL reference interferometer enable the quantification of this effect, and suggest this would set a minimum fractional uncertainty for this system of $\approx 7 \times 10^{-7}$.

6. Conclusions

A swept-frequency Michelson interferometer system has been developed and its performance verified by direct comparison with a displacement measuring interferometer. The best accuracy achieved is 3.2 parts in 10^6 for a distance of 8 m. The system could be improved by using a laser with a smoother and more linear scan and by using greater fringe subdivision.

Acknowledgements

The authors wish to acknowledge the support of the Department of Trade and Industry for this work, under NMS contract 2LMP/C01. In addition, the authors wish to acknowledge useful discussions with their colleagues at NPL. In particular they wish to thank Drs G P Barwood, J W Nunn and W R C Rowley (for his help in designing the electronics).

References

[1] Kikuta H., Iwata K. and Nagata R. Distance measurement by the wavelength shift of laser diode light *Appl. Opt.*, 1986, **25**, (17), 2976-80.

[2] Beheim G. and Fritsch K. Range finding using frequency-modulated laser diode *Appl. Opt.*, 1986, **25**, (9), 1439-42.

[3] Gerstner K. and Tschudi. T. New diode laser light source for absolute ranging two-wavelength interferometry *Opt. Eng.*, 1994, **33**, (8), 2962-6.

[4] Imai M. and Kawakita K. Optical-heterodyne displacement measurement using a frequency ramped laser diode *Opt. Commun.*, 1990, **78**, (2), 113-7.

[5] Kubota T., Nara M. and Yoshino T. Interferometer for measuring displacement and distance *Opt. Lett.*, 1987, **12**, (5), 310-2.

[6] Seta K. and Ward B.K. Interferometric absolute distance measurement utilizing a mode-jump region of a laser diode *Opt. Commun.*, 1990, **77**, (4), 275-8.

[7] Ohba R., Uehira I. and Kakuma S. Interferometric determination of a static optical path difference using a frequency swept laser diode *Meas. Sci. Technol.*, 1990, **1**, 500-4.

[8] Rovati L., Minoni U. and Docchio F. Dispersive white light combined with a frequency-modulated continuous-wave interferometer for high-resolution absolute measurements of distance *Opt. Lett.*, 1997, **22**, (12), 850-2.

[9] Zhu Y., Matsumoto H. and O'ishi T. Arm-length measurement of an interferometer using the optical-frequency-scanning technique *Appl. Opt.*, 1991, **30**, (25), 3561-2.

[10] Mahal V. and Arie A.. Distance measurements using two frequency-stabilized Nd:YAG lasers *Appl. Opt.*, 1996, **35**, (16), 3010-5.

[11] Barwood G.P., Gill P. and Rowley W.R.C. Laser diodes for length determination using swept-frequency interferometry *Meas. Sci. Technol.*, 1993, **4**, 988-94.

[12] Thiel J., Pfeifer T. and Hartman M. Interferometric measurement of absolute distances of up to 40 m *Measurement*, 1995, **16**, 1-6.

[13] Xiaoli D. and Katuo S. High-accuracy absolute distance measurement by means of wavelength scanning heterodyne interferometry *Meas. Sci. Technol.*, 1998, **9**, 1031-5.

[14] Barwood G.P., Gill P. and Rowley W.R.C. High-accuracy length metrology using multiple-stage swept-frequency interferometry with laser diodes *Meas. Sci. Technol.*, 1998, **9**, 1036-41.

[15] Birch K.P. and Downs M.J. An updated Edlén equation for the refractive index of air *Metrologia*, 1993, **30**, 155-62.

[16] Birch K.P. and Downs M.J. Correction to the updated Edlén equation for the refractive index of air *Metrologia,* 1994, **31**, 315-6.

[17] Littman M.G. and Metcalf H.J. Spectrally narrow pulsed dye laser without beam expander *Appl. Opt.,* 1978, **17**, (14), 2224-7.

[18] Barwood G.P., Gill P. and Rowley W.R.C A rubidium stabilised laser diode for interferometry *NPL Report MOM 85,* 1987.

[19] Barwood G.P., Gill P., Klein H.A. and Rowley W.R.C. Clearly resolved secular sidebands on the $^2S_{1/2}$-$^2D_{5/2}$ 674-nm clock transition in a single trapped Sr^+ ion *IEEE Trans. Instrum. Meas.,* 1997, **46**, (2), 133-6.

[20] Quinn T.J. Mise en Pratique of the Definition of the Metre (1992) *Metrologia,* 1994, **30**, (5), 523-41.

[21] Downs M.J., Birch K.P., Cox M.G. and Nunn J.W. Verification of a polarization-insensitive optical interferometer system with subnanometric capability *Prec. Eng.,* 1995, **17**, (1), 1-6.

[22] Downs M J and Raine K W 1979 An unmodulated bi-directional fringe-counting interferometer system for measuring displacement *Prec. Eng.* **1** 85-8

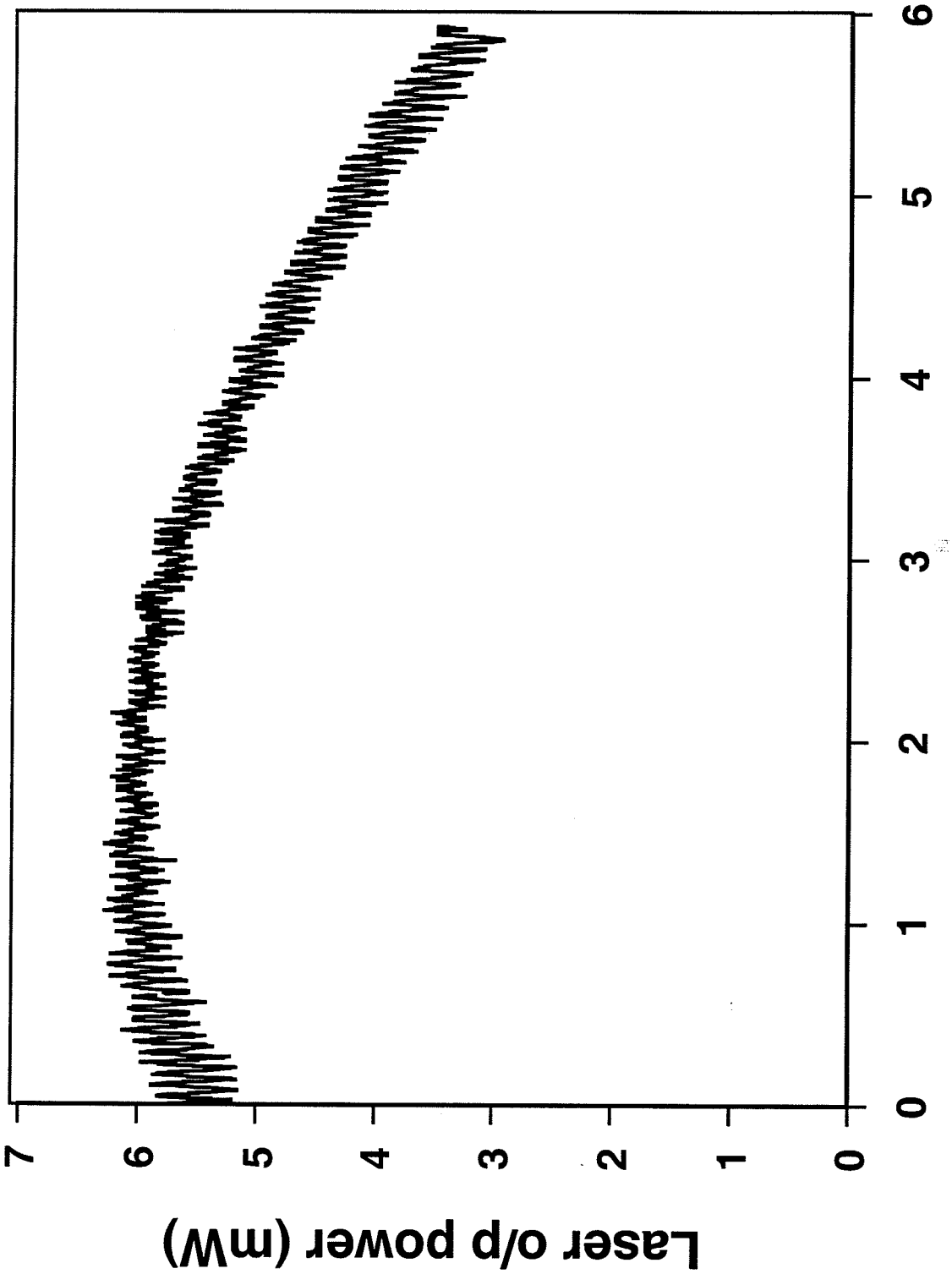

Figure 1. Plot of diode laser output power versus frequency during a scan; the start frequency is 468.8 THz.

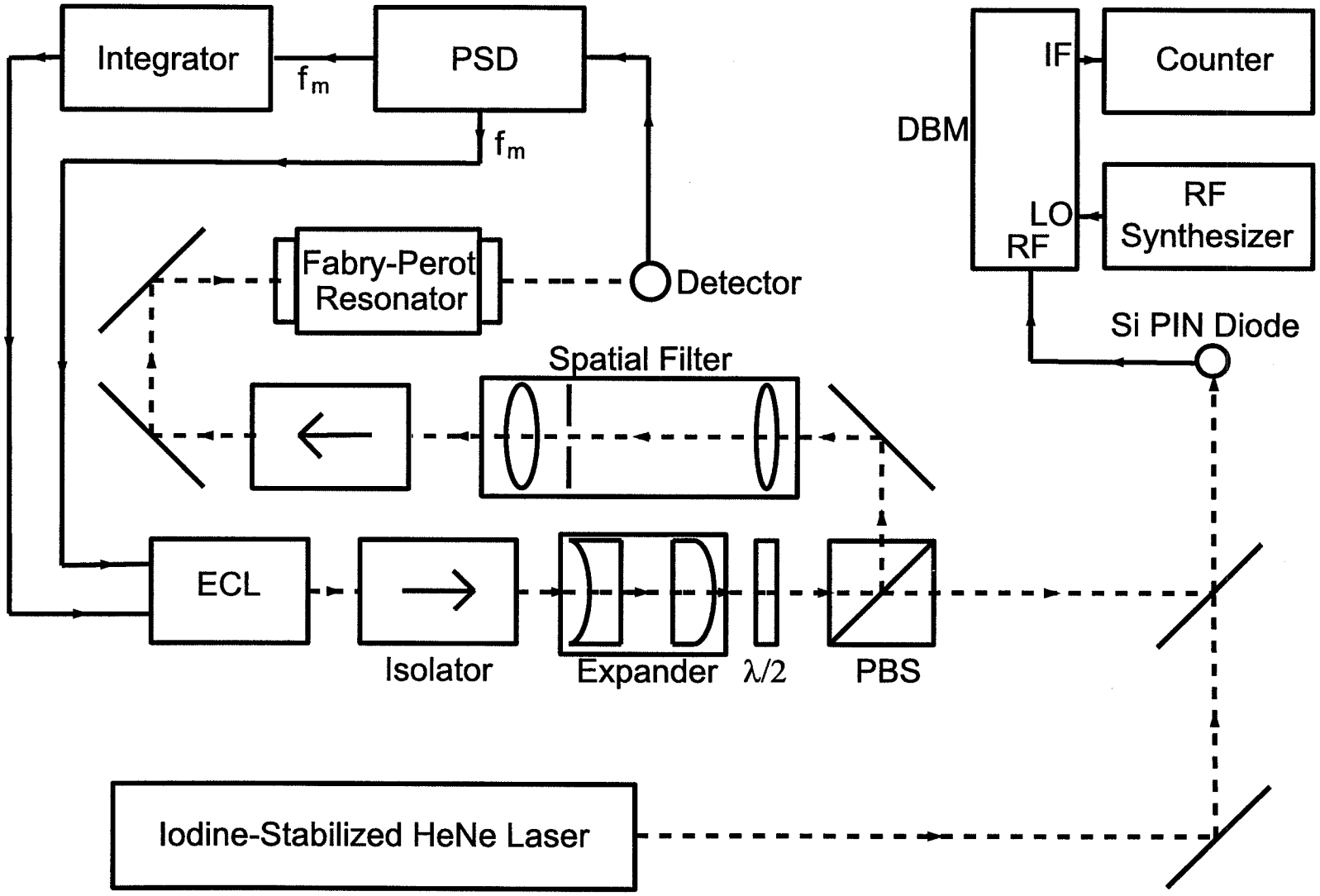

Figure 2. Experimental set-up for the measurement of the Fabry-Pérot free spectral range ν_{FSR}.
Key:- PSD ≡ phase sensitive detector, ECL ≡ extended cavity laser, DBM ≡ double-balanced mixer, PBS ≡ polarizing beamsplitter, λ/2 ≡ retardation plate, RF ≡ radio frequency, LO ≡ local oscillator, IF ≡ intermediate frequency.

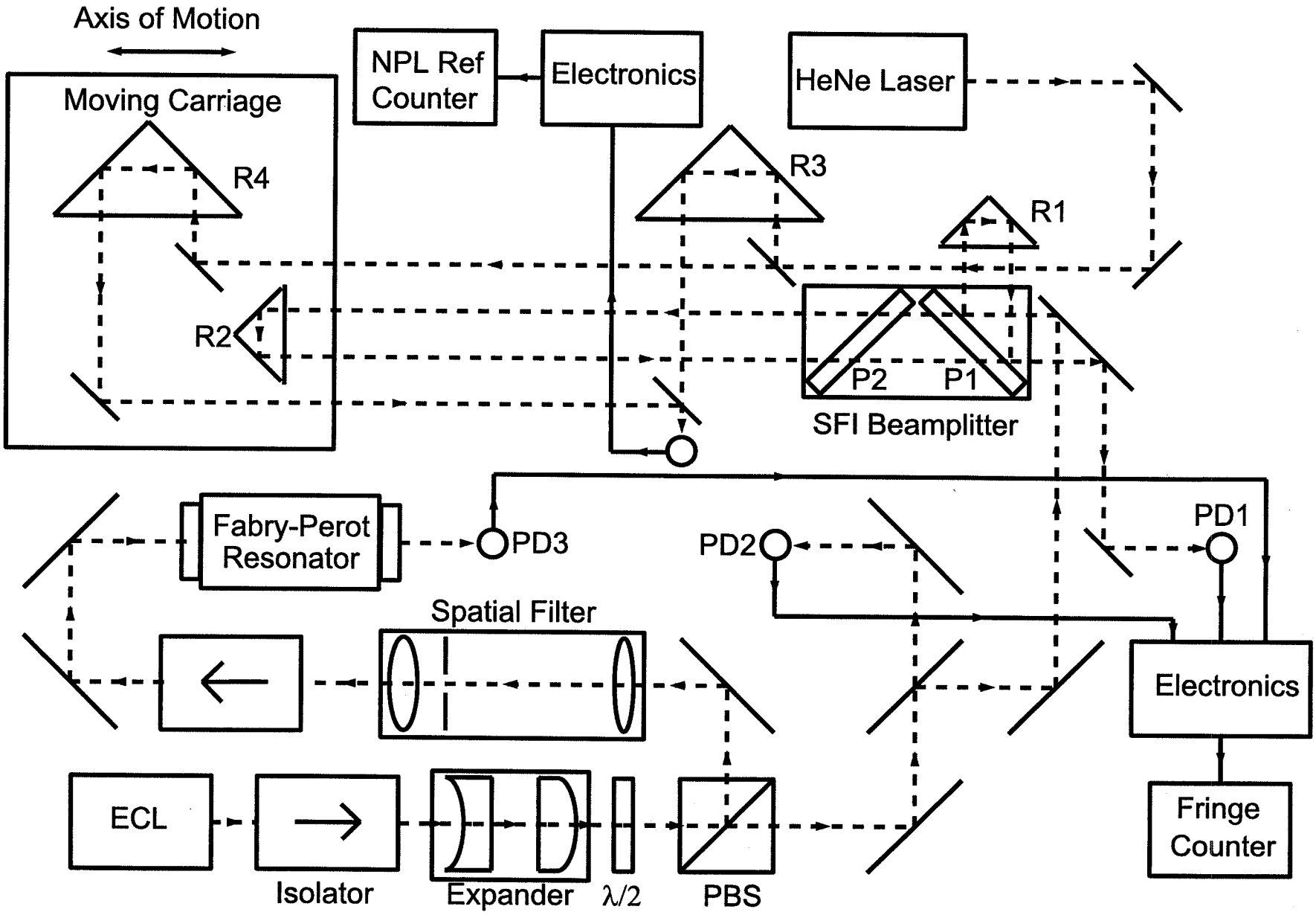

Figure 3. Experimental set-up for displacement measurement verification.
Key:- R ≡ retroreflector, PD ≡ photodiode, P ≡ interferometer plate, PBS ≡ polarizing beamsplitter, ECL ≡ extended cavity laser, λ/2 ≡ retardation plate, SFI Beamsplitter ≡ swept frequency interferometer beamsplitter assembly.

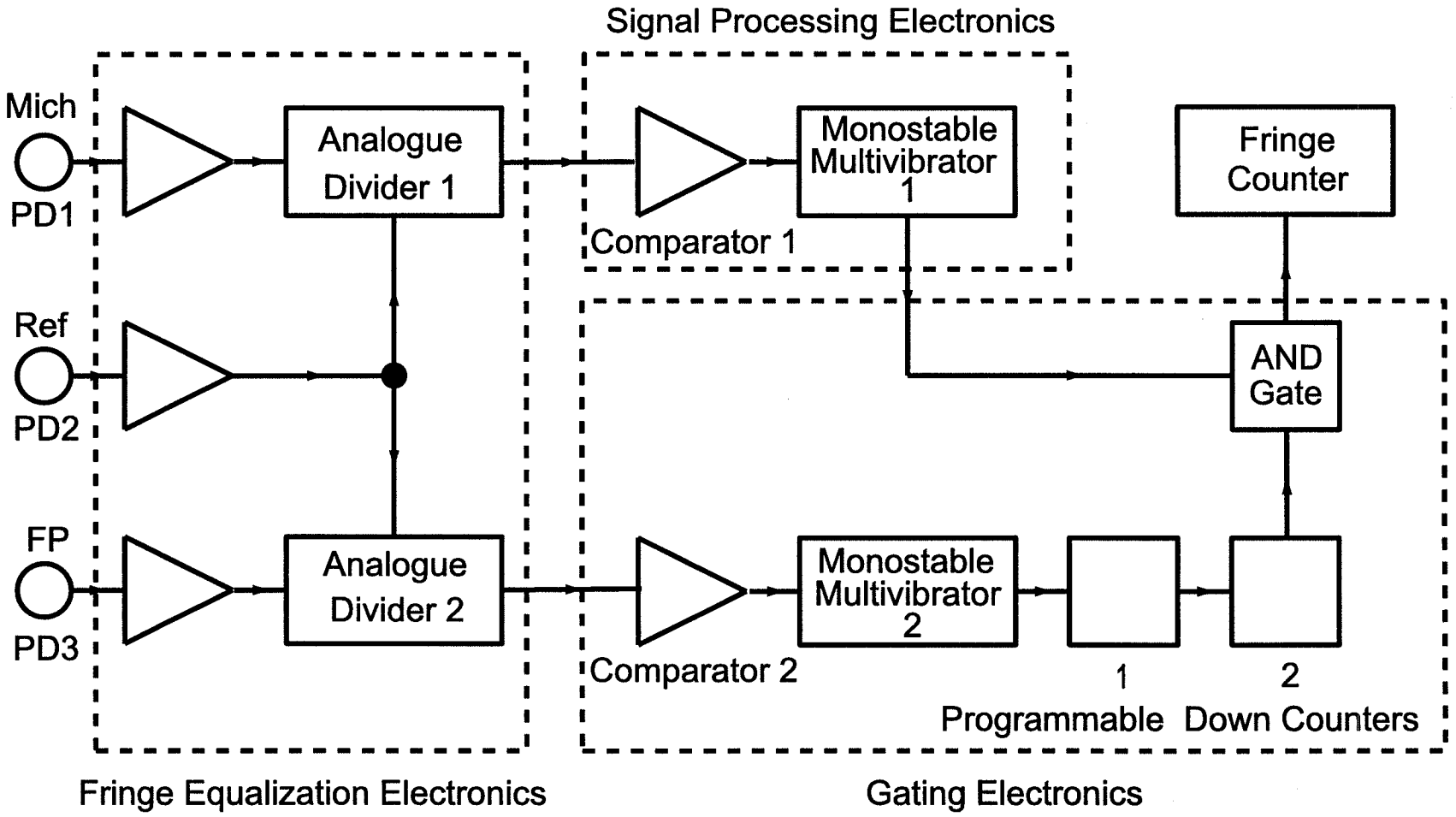

Figure 4. Simplified schematic of the swept-frequency interferometer electronics.

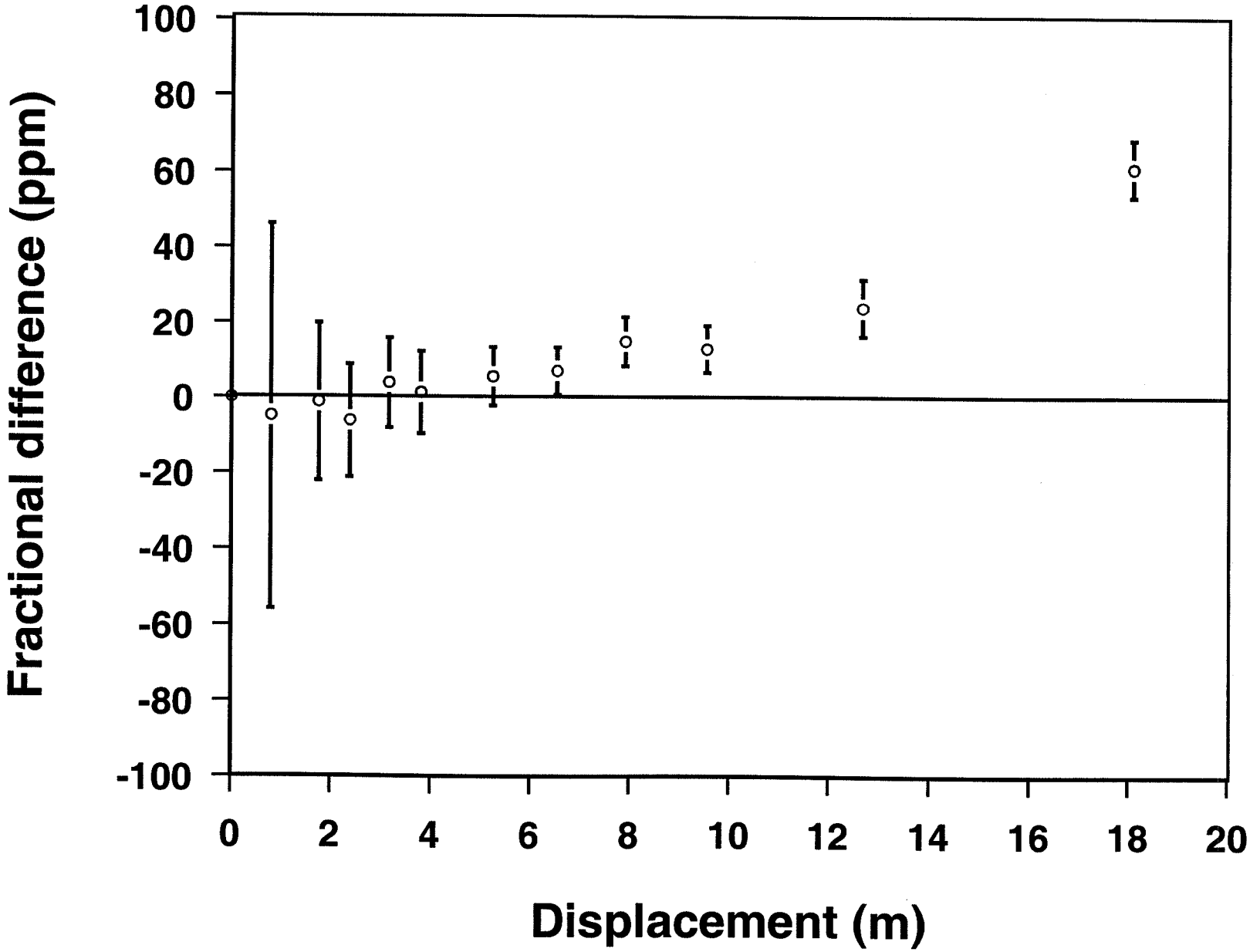

Figure 5. Plot of residuals (swept-frequency interferometer - NPL reference interferometer) versus displacement expressed as fractional uncertainties.